Inorg. Chem. **2005**, *44*, 3700–3708

High-Valent Imido Complexes of Manganese and Chromium Corroles

Nicola Y. Edwards,[†] Rebecca A. Eikey,[†] Megan I. Loring,[†] and Mahdi M. Abu-Omar*[,‡]

Department of Chemistry and Biochemistry, University of California, Los Angeles, California 90095, and Brown Laboratory, Department of Chemistry, Purdue University, 560 Oval Drive, West Lafayette, Indiana 47907

Received November 4, 2004

The oxidation reaction of M(tpfc) [M = Mn or Cr and tpfc = tris(pentafluorophenyl)corrole] with aryl azides under photolytic or thermal conditions gives the first examples of mononuclear imido complexes of manganese(V) and chromium(V). These complexes have been characterized by NMR, mass spectrometry, UV–vis, EPR, elemental analysis, and cyclic voltammetry. Two X-ray structures have been obtained for Mn(tpfc)(NMes) and Cr(tpfc)(NMes) [Mes = 2,4,6-$(CH_3)_3C_6H_2$]. Short metal–imido bonds (1.610 and 1.635 Å) as well as nearly linear M–N–C angles are consistent with triple M≡NR bond formation. The kinetics of nitrene [NR] group transfer from manganese(V) corroles to various organic phosphines have been defined. Reduction of the manganese(V) corrolato complex affords phosphine imine and Mn^{III} with reaction rates that are sensitive to steric and electronic elements of the phosphine substrate. An analogous manganese complex with a variant corrole ligand containing bromine atoms in the β-pyrrole positions, Mn(Br_8tpfc)(NAr), has been prepared and studied. Its reaction with PEt_3 is 250× faster than that of the parent tpfc complex, and its $Mn^{V/IV}$ couple is shifted by 370 mV to a more positive potential. The EPR spectra of chromium(V) imido corroles reveal a rich signal at ambient temperature consistent with Cr^{V}≡NR (d^1, $S = 1/2$) containing a localized spin density in the d_{xy} orbital, and an anisotropic signal at liquid nitrogen temperature. Our results demonstrate the synthetic utility of organic aryl azides in the preparation of mononuclear metal imido complexes previously considered elusive, and suggest strong σ-donation as the underlying factor in stabilizing high-valent metals by corrole ligands.

Introduction

Metal-mediated nitrogen atom transfer to olefins is an efficient method for preparing nitrogen-containing organic compounds such as aziridines and amines. This area of research has received considerable attention in recent years due to its promise in synthetic organic chemistry and in the preparation of natural products.[1,2] Groves and co-workers[3] reported the first activation of a (nitrido)manganese(V) porphyrin to effect the aziridination of cyclooctene in the presence of trifluoroacetic anhydride. This discovery stimulated the development of several catalytic[4] and stoichiometric[5] methods for metal-mediated [NR] group transfers. The active intermediate in these reactions is postulated to be a terminal metal imido species analogous to the isoelectronic metal oxo complexes prevalent in oxygen atom transfer (OAT) reactions and cytochrome P450 chemistry.[6] Hence, there is a continuing interest in characterizing metal imido complexes, particularly those of the first-row transition elements, and testing their reactivity.[7]

* Author to whom correspondence should be addressed. Fax: (765) 494-0238. E-mail: mabuomar@purdue.edu.
[†] University of California.
[‡] Purdue University.

(1) (a) Park, T. K.; Kim, I. J.; Hu, S.; Bilodeau, M. T.; Randolph, J. T.; Kwon, O.; Danishefsky, S. J. *J. Am. Chem. Soc.* **1996**, *118*, 11488. (b) Noda, K.; Hosoya, N.; Irie, R.; Ito, Y.; Katsuki, T. *Synlett* **1993**, 469.
(2) (a) Tanner, D.; Harden, A.; Johansson, F.; Wyatt, P.; Andersson, P. G. *Acta Chem. Scand.* **1996**, *50*, 361. (b) Tanner, D. *Angew. Chem., Int. Ed. Engl.* **1994**, *33*, 599.
(3) Groves, J. T.; Takahasi, T. *J. Am. Chem. Soc.* **1983**, *105*, 2073.
(4) See, for example: (a) Evans, D. A.; Faul, M. M.; Bilodeau, M. T. *J. Am. Chem. Soc.* **1994**, *116*, 2742. (b) Li, W.; Quan, R. W.; Jacobsen, E. N. *J. Am. Chem. Soc.* **1995**, *117*, 5889. (c) Halfen, J. A.; Hallman, J. K.; Schultz, J. A.; Emerson, J. P. *Organometallics* **1999**, *18*, 5435.
(5) (a) See, for example: DuBois, J.; Hong, J.; Carreira, E. M.; Day, M. W. *J. Am. Chem. Soc.* **1996**, *118*, 915. (b) Minakata, S.; Ando, T.; Nishimura, M.; Ryu, I.; Komatsu, M. *Angew. Chem., Int. Ed.* **1998**, *37*, 3392. (c) Minakata, S.; Ando T.; Nishimura, M.; Ryu I.; Komatsu, M. *Angew. Chem., Int. Ed.* **1998**, *110*, 3596 (d) DuBois, J.; Tomooka, C. S.; Hong, J.; Carreira, E. M. *J. Am. Chem. Soc.* **1997**, *119*, 3179.
(6) (a) Meunier, B. In *Metalloporphyrin Catalyzed Oxidations*; Montanary, F., Casella, L., Eds.; Kluwer Academic: Dordrecht, The Netherlands, 1994; Chapter 1. (b) Ortiz de Montellano, P. R. *Cyctochrome P450: Structure, Mechanism and Biochemistry*, 2nd ed.; Plenum Press: New York, 1995.

10.1021/ic0484506 CCC: $30.25
Published on Web 04/07/2005

Scheme 1

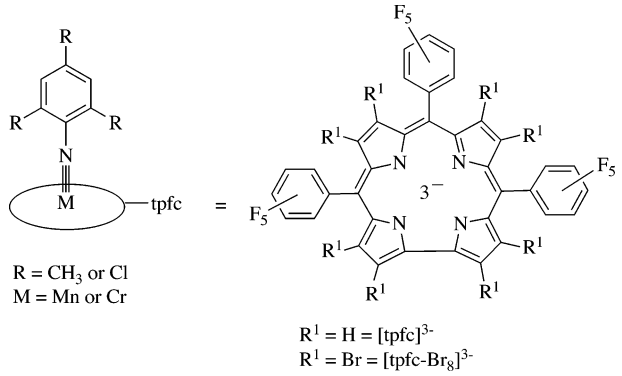

In 2002 we reported the synthesis and characterization of terminal imido manganese(V) complexes.[8] The ancillary ligand of choice was the tris(pentafluorophenyl)corrole (tpfc), which was employed by Gray and Gross to stabilize high-oxidation-state oxo and nitrido complexes.[9] The chemistry of high-oxidation-state manganese(V) oxo of the analogous corrolazine ligand has been investigated by Goldberg and co-workers.[10] Our manganese imido complexes were derived from the reaction of Mn^{III}(tpfc) and an aryl nitrene, which was generated by thermal or photochemical decomposition of the corresponding azide in a one-pot reaction. Although the imido ligand on manganese(V) transferred to phosphines, resulting in the formation of the phosphine imine adduct, it was not reactive toward olefins including electron-rich silyl enol ethers.

In this paper we provide a full account of the synthetic utility of aryl azides to generate imido corrole complexes of manganese and chromium (Scheme 1), electrochemical and spectroscopic characterizations of these novel complexes, and rate measurements on the reaction of manganese imido complexes with various organic phosphines.

Experimental Section

Materials. Preparation and handling of air-sensitive materials were carried out using standard vacuum line and glovebox techniques. Toluene and acetonitrile were predried using molecular sieves and distilled over CaH_2 prior to use. When required, solvents were deoxygenated via freeze−pump−thaw cycles. Deuterated solvents were purchased from Cambridge Isotopes and used without further purification. The syntheses of H_3(tpfc), Mn(tpfc), Mn(Br_8-tpfc), and Cr(tpfc)(py_2) followed previously described methods in the literature.[11] All other solvents and reagents were of reagent grade and used as received. Syntheses of Mn(tpfc)(NMes), Mes =2,4,6-$(CH_3)_3C_6H_2$ (**1**), and Mn(tpfc)(NAr), Ar = 2,4,6-$Cl_3C_6H_2$ (**2**), have been described previously.[8] All azides were prepared using the methodology of the Sandmeyer reaction or slight variations thereof.[12]

Caution! Aryl azides have been reported to detonate if heated to temperatures above 100 °C. While organic azides should be treated as potentially liable to detonate, particularly in the presence of heavy metals or acids, no problems were encountered in this study given the low concentrations used.

Physical Measurements. ^{1}H, ^{19}F, and ^{31}P NMR spectra were recorded on a Bruker ARX 400 spectrometer, MALDI mass spectra on a Voyager-DE STR (matrix, α-cyano-4-hydroxycinnamic acid; typical detailed instrument conditions are given in the Supporting Information alongside one of the spectra), and electronic absorption spectra on a Shimadzu UV-2501 spectrophotometer. Chemical shifts for ^{1}H were referenced relative to the solvent residual peak, and ^{31}P chemical shifts were referenced to the peak for 1% $P(OMe)_3$. Magnetic susceptibility was measured using Evan's method in $CDCl_3$ at 300 K.[13] Photolysis experiments were carried out using a Hanovia model 673A-0360 550 W medium-pressure mercury arc lamp. Elemental analyses were done by Desert Analytics Laboratory in Arizona. EPR spectra of Cr(tpfc)(NMes) (**6**) and Cr(tpfc)(NAr) (**7**) solutions ranging in concentration from 0.20 to 0.50 mM were taken in toluene at 4, 93, and 293 K on a Bruker EMX Spectrometer.

X-ray Crystal Determination of Cr(tpfc)(NMes)·C_7H_8 (6·C_7H_8). Crystals of **6**·C_7H_8 were obtained by the slow evaporation of a toluene solution at room temperature. A suitable crystal of dimensions 0.20 × 0.20 × 0.15 mm^3 was coated with Paratone N oil and subsequently mounted on a glass fiber that was placed under a nitrogen cold stream. The single-crystal diffraction data were collected at 100 K using a Bruker SMART 1000 CCD diffractometer employing graphite-monochromatized Mo Kα radiation (λ = 0.71073 Å). The SMART software was used for data acquisition, SAINT software for data extraction and reduction, and XPREP v6.12 software for the empirical absorption correction. Initial atomic positions were found by direct methods using XS followed by subsequent difference Fourier syntheses. The structure was solved and refined using the Bruker SHELTXTL (version 6.1) software package, using the monoclinic space group $P2(1)/c$ with $Z = 4$ for the formula unit $C_{53}H_{27}CrF_{15}N_5$. The final anisotropic full-matrix least-squares refinement on F^2 converged at R1 = 4.37%, wR2 = 9.1%, and a goodness-of-fit of 1.022. The largest peak on the final difference map was 0.389 $e^-/Å^3$. The calculated density for **6**·C_7H_8 ($C_{53}H_{27}CrF_{15}N_5$) is 1.604 Mg/m^3, and $F(000)$ is 2156 e^-. Crystallographic tables are given in the Supporting Information.

Electrochemical Studies. Cyclic voltammetry employed a Princeton Applied Research model 273A potentiostat with a glassy

(7) For a comprehensive review of metal nitrido and imido complexes, see: Eikey, R. A.; Abu-Omar, M. M. *Coord. Chem. Rev.* **2003**, *243*, 83. For examples of recently reported terminal imido complexes of the first-row transition metals, see: (a) Brown, S. D.; Betley, T. A.; Peters, J. C. *J. Am. Chem. Soc.* **2003**, *125*, 322. (b) Jenkins D. M.; Betley, T. A.; Peters, J. C. *J. Am. Chem. Soc.* **2002**, *124*, 11238. (c) Waterman, R.; Hillhouse, G. L. *J. Am. Chem. Soc.* **2003**, *125*, 13350. (d) Mindiola, D. J.; Hillhouse, G. L. *J. Am. Chem. Soc.* **2001**, *123*, 4623.

(8) Eikey, R. A.; Khan, S. I.; Abu-Omar, M. M. *Angew. Chem., Int. Ed.* **2002**, *41*, 3592.

(9) (a) Meier-Callahan, A. E.; Gray, H. B.; Gross, Z. *Inorg. Chem.* **2000**, *39*, 3605. (b) Gross, Z.; Golubkov, G.; Simkhovich, L. *Angew. Chem., Int. Ed.* **2000**, *39*, 4045. (c) Golubkov, G.; Bendix, J.; Gray, H. B.; Mahammed, A.; Goldberg, I.; DiBillio, A. J.; Gross, Z. *Angew. Chem., Int. Ed.* **2001**, *40*, 2132.

(10) (a) Mandimutsira, B. S.; Ramdhanie, B.; Todd, R. C.; Wang, H. L.; Zareba, A. A.; Czernuszewicz, R. S.; Goldberg, D. P. *J. Am. Chem. Soc.* **2002**, *124*, 15170. (b) Wang, S. H. L.; Mandimutsira, B. S.; Todd, R.; Ramdhanie, B.; Fox, J. P.; Goldberg, D. P. *J. Am. Chem. Soc.* **2004**, *126*, 18.

(11) tpfc: (a) Gross, Z.; Galili, N.; Saltsman, I. *Angew. Chem., Int. Ed.* **1999**, *38*, 1427. (b) Gross, Z.; Galili, N.; Simkhovich, L.; Saltsman, I.; Botoshansky, M.; Blaser, D.; Boese, R.; Goldberg, I. *Org. Lett.* **1999**, *1*, 599. *Mn(tpfc)*: (c) Gross, Z.; Golubkov, G.; Simkhovich, L. *Angew. Chem., Int. Ed.* **2000**, *39*, 4045. Mn(Br_8tpfc): (d) Golubkov, G.; Bendix, J.; Gray, H. B.; Mahammed, A.; Goldberg, I.; DiBilio, A. J.; Gross, Z. *Angew. Chem., Int. Ed.* **2001**, *40*, 2132. Cr(tpfc)(py_2): (e) Meirer-Callahan, A. E.; Di Bilio, A. J.; Simkhovich, L.; Mahammed, A.; Goldberg, I.; Gray, H. B.; Gross, Z. *Inorg. Chem.* **2001**, *40*, 6788.

(12) (a)Murata, S.; Abe, S.; Tomioka, H. *J. Org. Chem.* **1997**, *62*, 3055. (b) Leyva, E.; Munoz, D.; Platz, M. S., *J. Org. Chem.* **1989**, *54*, 5938.

(13) Evans, D. F. *J. Chem. Soc.* **1959**, 2003.

carbon working electrode, a platinum wire counter electrode, and a Ag/AgCl reference electrode with 0.1 M (n-Bu_4N)(PF_6) in CH_2Cl_2 as the supporting electrolyte. Potentials measured are with respect to the reference electrode but are corrected using the ferrocenium/ferrocene couple as measured under identical conditions. Solutions of the desired complexes **1**, **4**, **6**, and **7** (concentrations of approximately 1 mM) were prepared in dry, deoxygenated methylene chloride. Samples were prepared in the glovebox and loaded into the electrochemical cell using a gastight syringe. Solutions were purged with argon for an additional 5 min prior to data collection.

Kinetics of Imido Group Transfer from Mn(tpfc)(NAr) (2) and Mn(Br_8tpfc)(NAr) (5) to Various Phosphines. Solutions of **2** or **5** and various phosphines were prepared using dry, deoxygenated toluene in the glovebox. The concentrations of **2** and **5** were determined spectrophotometrically (**5**, log $\epsilon_{558} = 4.10$ M^{-1} cm^{-1}; **2**, log $\epsilon_{540} = 3.75$ M^{-1} cm^{-1}). Due to the instability of the aforementioned manganese complexes, solutions were freshly prepared prior to the start of each kinetic experiment. Rate measurements were carried out using either conventional UV−vis or a stopped flow reaction analyzer (Applied Photophysics SX.18MV) at 20.5 ± 0.5 °C.

The rates of reaction of **2** and **5** with various phosphines were measured by monitoring the formation of the phosphine imine adduct of manganese(III) at approximately 475 nm (varies from 470 to 485 nm depending on the phosphine) under pseudo-first-order conditions with a phosphine concentration at least 10-fold in excess of the manganese complex. Plots of the pseudo-first-order rate constants (k_ψ) versus phosphine concentration were linear, and the slopes afforded second-order rate constants (k_1).

Typical Reaction Conditions for the Preparation of Phosphine Imine Adducts Mn(tpfc)(NArPPh$_3$) and Mn(tpfc)(NArPCy$_3$). A solution of **2** (25 mg, 24 μmol) and a stoichiometric amount of PR_3 in 5 mL of toluene was stirred at room temperature under an argon atmosphere. The solution turned green in a matter of minutes. The progress of reaction was followed by UV−vis until complete conversion to the phosphine imine adduct. The following are data for Mn(tpfc)(NArPPh$_3$). MALDI MS: $m/z = 1303$ $(M - 2H)^+$ with correct isotope pattern (see the Supporting Information). UV−vis (toluene): λ_{max}/nm = 396, 416, 475, 609. The following are data for Mn(tpfc)(NArPCy$_3$). MALDI MS: $m/z = 1322$ $(M - H)^+$ with correct isotope pattern (see the Supporting Information). UV−vis (toluene): λ_{max}/nm = 389, 414, 470, 611. Attempts to obtain single crystals from these solutions over prolonged periods of time were not successful. Subjecting the reaction mixture to TLC showed a spot corresponding to phosphine imine $NArPR_3$ by comparison to an authentic sample. Preparative TLC yielded starting (tpfc)Mn^{III} and phosphine imine $NArPR_3$ in essentially quantitative yield (≥90%).

Mn(tpfc)(NAr′), Ar′ = 2,6-$Cl_2C_6H_3$ (3). 2,6-Dichlorophenyl azide (40 mg, 0.21 mmol) was added to a stirring solution of Mn(tpfc) (13 mg, 15.3 μmol) in acetonitrile (dry, deoxygenated, 6 mL) under argon. The solution was photolyzed until TLC analysis showed complete consumption of starting material (approximately 3 days). The resulting burgundy solution was evaporated to dryness under vacuum and chromatographed on silica gel (60 Å, 12:1 pentane/ether). **3** was isolated as a fragile burgundy microcrystalline solid (7 mg, 7 μmol, 45%). ^{1}H NMR ($CDCl_3$, 400.1 MHz, 300 K): δ 9.12 (d, $J = 4.3$ Hz, 2 H), 8.83 (d, $J = 3.6$ Hz, 2 H), 8.66 (d, $J = 3.7$ Hz, 2 H), 8.58 (d, $J = 3.9$ Hz, 2 H), 6.46 (t, $J = 7.4$ Hz, 1 H), 6.10 (d, $J = 8.0$ Hz, 2 H). ^{19}F NMR ($CDCl_3$, 400.1 MHz, 300 K): δ −137.29 (m, 2 F), −137.41 (m, 2 F), −137.75 (m, 2 F), −153.26 (m, 3 F), −162.04 to −162.24 (m, 6 F). UV−vis (toluene): λ_{max}/nm (rel abs) = 376 (2.8), 541 (1.0). MALDI MS (rel intens) [assignment]: m/z 1007 (19) $[M]^+$, 864 (7) $[M - Ar']^+$, 848 (100) $[M - NAr']^+$.

Mn(Br_8tpfc)(NMes) (4). Method A. Mesityl azide (51.5 mg, 0.317 mmol) was added to a stirring solution of Mn(Br_8tpfc) (21.4 mg, 14.5 μmol) in 8 mL of dry toluene under argon. The reaction mixture was heated to 85 °C until TLC analysis showed complete consumption of starting material (approximately 5 h) and evaporated to dryness under vacuum. Chromatography as described for **3** followed by anaerobic recrystallization from hexanes and methylene chloride afforded **4** (9 mg, 38%) as a burgundy microcrystalline solid.

Method B. Mesityl azide (9.4 mg, 58.3 μmol) was added to a stirring solution of Mn(Br_8tpfc) (4 mg, 2.7 μmol) in acetonitrile (dry, deoxygenated, 2 mL) under argon. The reaction mixture was photolyzed until TLC analysis showed complete conversion of starting material (approximately 3−4 days) and evaporated to dryness under vacuum. Chromatography afforded **4** (1.5 mg, 38% yield) as a burgundy crystalline solid. ^{1}H NMR ($CDCl_3$, 400.1 MHz, 300 K): δ 5.72 (s, 2 H), 1.69 (s, 3 H), −0.39 (s, 6 H). ^{19}F NMR ($CDCl_3$, 400.1 MHz, 300 K): δ −136.75 (m, 2 F), −136.92 (m, 1 F), −138.68 (m, 3F), −152.08 (m, 3 F), −163.0 to −163.43 (m, 6 F). UV−vis (toluene): λ_{max}/nm (log ϵ) = 426 (4.65), 549 (4.10), 791(2.55). UV−vis (CH_2Cl_2): λ_{max}/nm (log ϵ) = 424 (4.82), 546 (4.27), 760 (3.04). MALDI MS (rel intens) [assignment]: m/z 1612 (40) $[M]^+$, 1479 (100) $[M - NMes]^+$. Anal. Calcd for $MnF_{15}N_5C_{60}H_{27}Br_8$ (**4**·$2C_7H_8$): C, 40.08; H, 1.50; N, 3.90. Found: C, 40.00; H, 1.42; N, 3.94.

Mn(Br_8tpfc)(NAr) (5). 2,4,6-Trichlorophenyl azide (40.5 mg, 0.182 mmol) was added to a stirring solution of Mn(Br_8tpfc) (14 mg, 9.46 μmol) in acetonitrile (dry, deoxygenated, 5 mL) under argon. The reaction mixture was photolyzed for 6 days. The resulting brown solution was evaporated to dryness under vacuum, washed with acetonitrile, dissolved in CH_2Cl_2, and chromatographed (basic alumina activity IV, CH_2Cl_2) to yield **5** (13.5 mg, 85%) as a burgundy microcrystalline solid. ^{1}H NMR ($CDCl_3$, 400.1 MHz, 300 K): δ 6.27 (s, 2 H). ^{19}F NMR ($CDCl_3$, 400.1 MHz, 300 K): δ −136.91 (m, 2 F), −137.14 (d, 1 F), −138.17 (m, 3 F), −151.75 (m, 3 F), −162.75 to −163.16 (m, 6 F). UV−vis (toluene): λ_{max}/nm (rel abs) = 419 (3.2), 558 (1.0). MALDI MS (rel intens) [assignment]: m/z 1479 (100) $[M - NAr]^+$.

Cr(tpfc)(NMes) (6). Method A. Mesityl azide (18.3 mg, 0.114 mmol) was added to a stirring solution of Cr(tpfc)$(py)_2$ (11.6 mg, 11.5 μmol) in 8 mL of dry toluene under argon. The reaction mixture was refluxed until TLC analysis showed complete consumption of starting material (approximately 3.5 h) and evaporated to dryness under vacuum. Chromatography as described for **3** followed by aerobic recrystallization from pentane and toluene afforded **6** (7.2 mg, 62%) as a burgundy semicrystalline solid.

Method B. Mesityl azide (77 mg, 0.478 mmol) was added to a stirring solution of Cr(tpfc)$(py)_2$ (12 mg, 12 μmol) in acetonitrile (dry, deoxygenated, 4 mL) under argon. The reaction mixture was photolyzed for approximately 9−10 days and evaporated to dryness under vacuum. Chromatography as described for **3** followed by aerobic recrystallization from pentane and toluene afforded **6** (2 mg, 17%) as a burgundy semicrystalline solid. UV−vis (CH_3CN): λ_{max}/nm (log ϵ) = 530 (2.97), 408 (3.07). MALDI MS (rel intens) [assignment]: m/z 979 (100) $[M]^+$, 845 (100) $[M - NMes]^+$. μ_{eff} ($CDCl_3$, 300 K) = 1.90 μ_B. Anal. Calcd for $CrF_{15}N_5C_{52}H_{29}$ (**6**·$^1/_2C_5H_{12}$·$^1/_2C_7H_8$): C, 58.88; H, 2.76; N, 6.60. Found: C, 59.06; H, 3.26; N, 5.86.

Cr(tpfc)(NAr) (7). Method A. 2,4,6-Trichlorophenyl azide (47 mg, 0.211 mmol) was added to a stirring solution of Cr(tpfc)$(py)_2$

(18 mg, 18 μmol) in 8 mL of dry toluene and refluxed under argon for 24 h. The solvent was removed under vacuum and chromatographed as described for **3**. This was followed by aerobic recrystallization from pentane and toluene to yield **7 (**7.1 mg, 38%**)** as a burgundy semicrystalline solid.

Method B. 2,4,6-Trichlorophenyl azide (38 mg, 0.17 mmol) was added to a stirring solution of Cr(tpfc)$(py)_2$ (10 mg, 10 μmol) in acetonitrile (dry, deoxygenated, 5 mL) under argon. The reaction mixture was photolyzed for approximately 4−5 days. Chromatography as described for **3** followed by aerobic recrystallization from pentane and toluene afforded **7** as a burgundy semicrystalline solid. UV−vis (CH_3CN): λ_{max}/nm (log ϵ) = 536 (4.05), 391 (4.58). MALDI MS (rel intens) [assignment]: *m/z* 1040 (95) $[M]^+$, 845 (100) $[M - NAr]^+$. μ_{eff} ($CDCl_3$, 300 K) =1.93 μ_B. Anal. Calcd for $CrCl_3F_{15}N_5C_{49}H_{20}$ (**7**·$^1/_2C_5H_{12}$·$^1/_2C_7H_8$): C, 52.45; H, 1.80; N, 6.24. Found: C, 52.22; H, 2.28; N, 5.58.

Results and Discussion

Synthesis, Characterization and Reactivity of Manganese(V) Imido Corrole Complexes. The facile synthetic route to the first well-characterized terminal imido complex of manganese(V) has been communicated.[8] This complex was most likely derived from the reaction of Mn(tpfc) and mesityl nitrene generated from thermal or photochemical decomposition of the corresponding azide.[14] This synthetic methodology has been successfully employed in the synthesis of manganese(V) imido complexes derived from other aryl azides, namely, 2,4,6-trichlorophenyl and 2,6-dichlorophenyl azides. Furthermore, the brominated corrole ligand Br_8tpfc can be used instead of tpfc to enhance the activity of the metal center. The imido complexes were purified by flash chromatography and characterized by NMR, mass spectrometry, and elemental analyses. Yields are moderate, and reactions were generally done thermally whenever possible due to reduced time of reaction, higher product yields, and amenability to larger scales.

Reactions with phosphines as well as lack of reaction with organic acids such as trifluoroacetic acid (TFA) and methyl iodide are a testimony to the electrophilicity of the NR (imido) group in these complexes. In the case of Mn(tpfc)(NMes) (**1**), which is stable indefinitely under argon, formation of the phosphine imine was complete after a day at 85 °C.[8] This is in startling contrast to the Mn(tpfc)(NAr) (**2**), which must be stored in the freezer in the glovebox to retard its decomposition, reacting with phosphines on the time scale of minutes at room temperature. However, the imido species are not reactive toward olefins of any kind including the electron-rich silyl enol ethers.

Kinetic Studies of NR Group Transfer from Mn(tpfc)(NAr) to Various Organic Phosphines. Rates of reduction of **2** by a series of phosphines that vary widely in steric and electronic properties have been measured. The progress of reaction was monitored at approximately 470 nm (which varies in the range 470−485 nm depending on the phosphine), corresponding to the formation of the phosphine imine adduct. The UV−vis spectra of **2** and its reaction product with PPh_3, Mn^{III}(tpfc)($NArPPh_3$), are shown in Figure 1A. In addition to the pronounced LMCT band at 475 nm, other key features are the splitting of the Soret band and the shift of the Q-band upon product formation. These are indicative of a change in oxidation state and manifested by a change in color from burgundy to green. It is worth noting that the UV−vis spectrum of the resulting phosphine imine adduct, Mn^{III}(tpfc)($NArPPh_3$), is distinguishable from the UV−vis spectra of Mn^{III}(tpfc) and Mn^{III}(tpfc) with excess PPh_3 (Figure 1B). The addition of a large excess of PPh_3 had very subtle effects on the UV−vis spectrum of Mn(tpfc). In comparison, the spectra of the reaction product of **2** and PR_3 yielded distinct spectra with variable maxima between 470 and 485 nm depending on the identity of the organic phosphine. Furthermore, a peak corresponding to the mass of the manganese phosphine imine adduct with the correct isotope pattern was detected by MALDI-TOF MS in reaction mixtures of all phosphines. Three representative mass spectra are shown in the Supporting Information for (tpfc)Mn($NArPPh_3$), (tpfc)Mn($NArP(4\text{-}FC_6H_4)_3$), and (tpfc)Mn($NArPCy_3$). Therefore, on the basis of UV−vis and mass spectrometry results, we conclude that the initial product from the reaction of (imido)manganese(V) corrole complexes

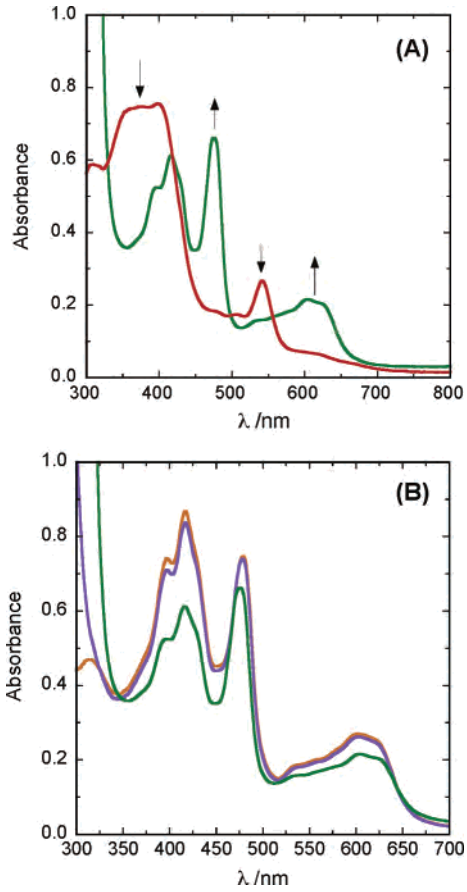

Figure 1. UV−vis spectra in toluene of (A) 40 μM **2** (red) and its reaction product with 400 μM PPh_3, Mn^{III}(tpfc)($NArPPh_3$) (green), and (B) 40 μM Mn^{III}(tpfc) (orange) and the same compound in the presence of 400 μM PPh_3 (purple) compared to the product from the reaction of **2** with PPh_3, Mn^{III}(tpfc)($NArPPh_3$) (green).

(14) For examples of aryl azides as nitrene sources in the formation of metal imido complexes, see: (a) Hillhouse, G. L.; Bercaw, J. E. *Organometallics* **1982**, *1*, 1025. (b) Antonelli, D. M.; Schaefer, W. P.; Parkin, G.; Bercaw, J. E. *J. Organomet. Chem.* **1993**, *462*, 213. (c) La Monica, G.; Cenini, S. *J. Chem. Soc., Dalton Trans.* **1980**, 1145.

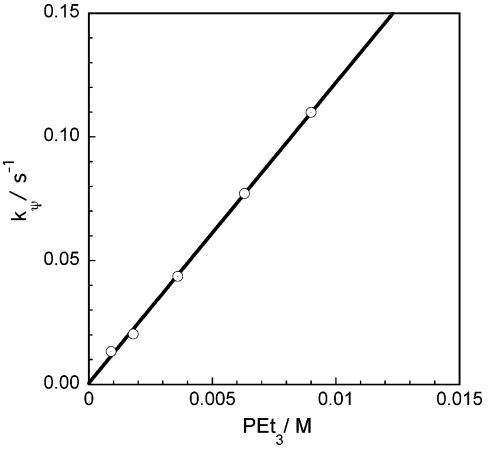

Figure 2. A plot of the observed pseudo-first-order rate constant (k_ψ) versus [PEt_3] for the reaction of PEt_3 with **2** at 20.5 ± 0.5 °C.

with phosphines is the manganese(III) phosphine imine adduct.

The reaction of manganese(V) corrole complexes with phosphines to afford manganese(III) phosphine imine (Mn^{III} ← N(Ar)═PR_3) is taken to represent complete imido (NAr) group transfer from the metal to phosphorus. The starting manganese(V) imido is diamagnetic, and the product is paramagnetic. The UV−vis spectral features of the reaction (see above) are consistent with the assigned oxidation states. Furthermore, phosphine imine does not react with manganese(III) corrole to give manganese(V) imido.

Product formation was authenticated for the reaction with PPh_3. Addition of a slight excess of PPh_3 to **2** resulted in the formation of a green reaction mixture within minutes. Purification via preparative TLC subsequently led to the isolation of Mn(tpfc) and the free phosphine imine in essentially quantitative yields. The latter was identified by mass spectrometry and ^1H and ^{31}P NMR via comparison to an authentic sample prepared independently from the reaction of phosphine and aryl azide.[15]

It should be noted that the use of (imido)manganese(V) corrole complexes in the preparation of phosphine imines would have no practical value whatsoever, nor does it constitute by any means the purpose for this investigation. Phosphine imines can be synthesized conveniently from the reaction of phosphine and azide (the Staudinger reaction).[15] Nevertheless, the point of this kinetic study is to gain insight into the reactivity and reaction mechanisms of novel terminal imido complexes of manganese.

Reduction of **2** by trialkyl- and alkylarylphosphines displayed single-exponential time profiles under pseudo-first-order conditions with phosphine concentrations at 10-fold or more excess. The observed rate constant, k_ψ, varied linearly with phosphine concentration in accordance with an overall second-order rate law: $-d[\mathbf{2}]/dt = k_1[\mathbf{2}][PR_3]$. A representative plot for the reaction with PEt_3 is shown in Figure 2. Second-order rate constants (k_1) determined from the slopes of k_ψ versus [PR_3] plots are listed in Table 1.

In contrast to trialkyl- or arylalkylphosphines, reduction of **2** by triarylphosphines displayed complex kinetics. Biphasic time profiles were obtained under pseudo-first-order

Table 1. Second-order Rate Constants (k_1) for the Reaction of Organic Phosphines with **2** along with Tolman's Steric (Cone Angle/deg) and Electronic (χ/cm^{-1}) Parameters

phosphine	k_1[a]/M^{-1} s^{-1}	cone angle/deg	χ/cm^{-1}
P(*p*-FC_6H_4)$_3$	0.062(6)	145	15.7
PPh_3	0.71(5)	145	13.25
PPh_2Et	1.09(2)	140	11.3
P(*p*-Tol)$_3$	0.78(6)	145	10.5
PEt_3	12.1(2)	132	6.3
PCy_3	0.0480(2)	170	1.4

[a] In toluene at 20.5 ± 0.5 °C.

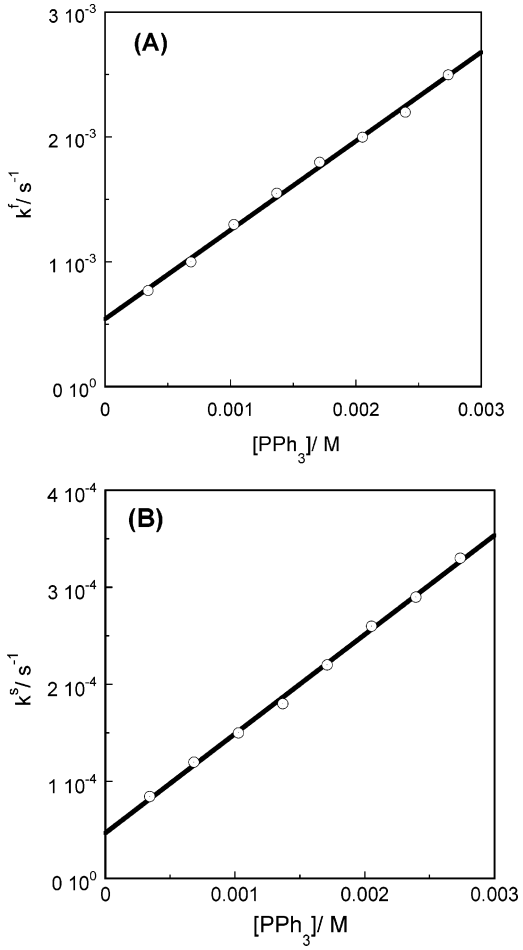

Figure 3. Dependence of the fast (k^f) and slow (k^s) stages on PPh_3 concentration for its reaction with **2**.

conditions. The data were fit to a nonlinear least-squares biexponential equation. The observed rate constants, k^f (fast) and k^s (slow), varied linearly with the phosphine concentration and featured discernible nonzero *y* intercepts. Typical plots of k^f and k^s are illustrated in Figure 3 for the reaction with PPh_3. The *y* intercepts cannot be due to complex decomposition since, over the time scale of these reactions, the manganese complex is stable. Furthermore, a study of reaction kinetics based on a series of phosphines with different substituents in the para position of the aryl ring

(15) (a) Staudinger, H.; Meyer, J. *Helv. Chim. Acta* **1919**, *2*, 635. (b) Gololobov, Y. G.; Zhmurova, I. N.; Kasukhin, L. F. *Tetrahedron* **1981**, *37*, 437−472. (c) Wei, P.; Chan, K. T. K.; Stephan, D. W. *Dalton Trans.* **2003**, 3804. (d) Masuda, J. D.; Walsh, D. M.; Wei, P.; Stephan, D. W. *Organometallics* **2004**, *23*, 1819.

Scheme 2. Ligand-Assisted Mechanism Which May Account for the Observed Biphasic Kinetics with Triarylphosphines

$$(\text{tpfc})\text{Mn}^{\text{V}}(\text{NAr}) \xrightarrow{k_1^B[\text{PPh}_3]} (\text{tpfc})(\text{PPh}_3)\text{Mn}^{\text{V}}(\text{NAr}) \xrightarrow{k_2^B[\text{PPh}_3]} (\text{tpfc})(\text{PPh}_3)\text{Mn}^{\text{III}}(\text{N(Ar)}(\text{PPh}_3))$$

was attempted. In the case of P(*p*-Tol)$_3$, rate constants for both fast and slow stages were comparable to those of unsubstituted PPh_3, and the reaction with P(*p*-FC_6H_4)$_3$ displayed a significant *y* intercept. Thus, no Hammett correlation can be drawn from these findings. Since the fast stage accounts for the bulk of absorbance change and is consistent with the reduction of manganese(V) to manganese(III), the rate constants from the fast stage (k^f) were taken to represent NR group transfer to triarylphosphines and are presented in Table 1. Similar biphasic and complex kinetics have been observed for imido transfer from a ruthenium porphyrin to triarylphosphines.[16] One possible assignment of the slow stage is ligand dissociation of the resulting phosphine imine on manganese(III) assisted or catalyzed by phosphine substrate. However, the physical basis of a substrate-independent pathway (i.e., *y* intercepts in Figure 3) cannot be accounted for by this proposal. Additionally, a mechanism in which the arylphosphine complex replaces the phosphine imine adduct is not supported by the observation that the resulting spectrum of the product at the end of the kinetic run is distinct from that of Mn(tpfc) and phosphine (Figure 1B).

Biphasic kinetics might be the result of a ligand-assisted pathway in which the phosphine substrate coordinates trans to the imido ligand prior to NR transfer (Scheme 2). To explore the role of trans-coordinating ligands on the rate of reaction, experiments were carried out with added pyridine, which was varied in concentration between 5 and 40 equiv with respect to **2**. No difference in reaction rates was detected, and hence, a ligand-assisted pathway is not fully supported.

Steric and Electronic Effects of Phosphines. Table 1 contains rate constants for several phosphine substrates along with Tolman's electronic and steric parameters.[17] The electronic map (Figure 4) demonstrates that phosphine imine formation is favored by more nucleophilic phosphines with the exception of PCy_3 in which activity is dictated by a steric effect. Log k_1 decreases in the order PEt_3 ($\chi = 6.3$ cm^{-1}), PPh_2Et ($\chi = 11.3$ cm^{-1}), PPh_3 ($\chi = 11.3$ cm^{-1}), and P(*p*-FC_6H_4)$_3$ ($\chi = 15.7$ cm^{-1}). Rate constants obtained span over 2 orders of magnitude. Phosphine imine formation is clearly favored by less sterically hindered phosphines as measured by their cone angles in degrees (Figure 5, steric map). Log k_1 increases in the order PCy_3 (170°), PPh_3 and P(*p*-Tol)$_3$ (145°), PPh_2Et (140°), and PEt_3 (132°). P(*p*-FC_6H_4)$_3$, isosteric with PPh_3 and P(*p*-Tol)$_3$, is the mere exception to this trend. Its relatively small value of k_1 reflects its intrinsically low nucleophilicity. Both factors together, the sterics and electronics of phosphines, govern the rate of phosphine addition to the manganese(V) imido in **2** to afford the manganese(III) phosphine imine.

(16) Leung, W.-H.; Hun, T. S. M.; Hou, H.-W.; Wong, K.-Y. *J. Chem. Soc., Dalton Trans.* **1997**, 237.
(17) Tolman, C. A. *Chem. Rev.* **1977**, *77*, 313.

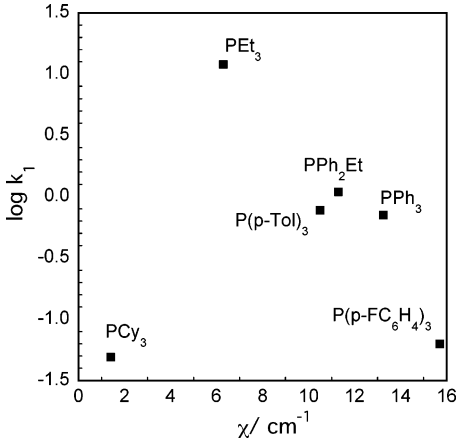

Figure 4. Electronic map (log k_1 vs Tolman's electronic parameter χ) for the reaction of phosphines with **2**.

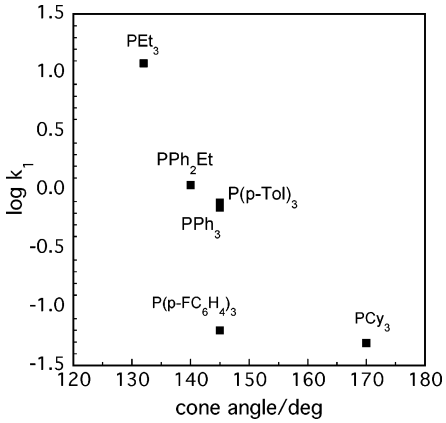

Figure 5. Steric map (log k_1 vs Tolman's cone angle) for the reaction of phosphines with **2**.

Tuning the Reactivity via Ligand Modification. This work and previous studies done on both porphyrin and corrole complexes[9,18] gave rise to the speculation that more electron-deficient imido corrole complexes are potential stoichiometric nitrogen atom transfer agents to olefins. Toward this end, analogues of the imido species based on corrole ligands with Br atoms in the β-pyrrole positions of the macrocycle were synthesized.

To directly measure the electrophilicity around the metal center and hence its reactivity, electrochemical properties of the imido complexes were investigated via cyclic voltammetry (Table 2). The cyclic voltammograms of the imido complexes were measured relative to the Ag/AgCl electrode in 0.10 M (*n*-Bu_4N)(PF_6) in CH_2Cl_2 at ambient temperature. They feature two one-electron reversible redox processes: a ligand-based oxidation corresponding to the corrole/corrole π-radical cation (tpfc/tpfc$^{\bullet+}$) couple and a metal-based reduction corresponding to the metal(V/IV) couple. Peak assignments were based on comparison to the (tpfc)Cr(V)O complex.[9] Reversibility was established by the near-unity value of the cathodic and anodic peak current intensities and

(18) For brominated porphyrins and corroles, see, for example: (a) Grinstaff, M. W.; Hill, M. G.; Birbaum, E. R.; Schaefer, W. P.; Labinger, J. A.; Gray, H. B. *Inorg. Chem.* **1995**, *34*, 4896. (b) Mahammed, A.; Meier-Callahan, A. E.; Gross, Z. *J. Am. Chem. Soc.* **2003**, *125*, 1162. For fluorinated corroles, see: Lui, H.-Y.; Lai, T.-S.; Yeung, L.-L.; Chang, C. K. *Org. Lett.* **2003**, *5*, 617.

Table 2. Redox Potentials (V) vs Ag/AgCl for Metal(V) Imido Corrole Complexes[a]

complex	$E_{1/2}$(tpfc/tpfc$^{+\cdot}$)	$E_{1/2}$($M^{5+/4+}$)	complex	$E_{1/2}$(tpfc/tpfc$^{+\cdot}$)	$E_{1/2}$($M^{5+/4+}$)
Mn(tpfc)(NMes) (**1**)	1.21	−0.36	Cr(tpfc)(NAr) (**7**)	1.29	−0.13
Mn(Br_8tpfc)(NMes) (**4**)	1.67	0.01	Cr(tpfc)(O)[b]	1.25	0.11
Cr(tpfc)(NMes) (**6**)	1.31	−0.47			

[a] Redox potentials were obtained from $E_{1/2} = (E_{pa} + E_{pc})/2$ and were corrected by the potential of the ferrocenium/ferrocene couple. Cyclic voltammograms were obtained in CH_2Cl_2 with 0.1 M (n-Bu_4N)(PF_6) as the supporting electrolyte at 298 K. The scan rate was 25 mV s^{-1}. [b] Reference 9a.

stoichiometry by the comparability of the peak current to that of the ferrocene/ferrocenium redox couple of the same concentration under identical conditions.

Comparisons of the electrochemical measurements between the imido species based on the tpfc and Br_8tpfc ligand systems were done using those derived from mesityl azide due to their stability. However, comparisons of rate measurements were done using imido species derived from trichlorophenyl azide due to their enhanced reactivity. In the cyclic voltammogram of **1**, the tpfc/tpfc$^{\bullet+}$ and the $Mn^{V/IV}$ couples occur at potentials of 1.21 and −0.36 V, respectively. In the case of **4**, the tpfc/tpfc$^{\bullet+}$ redox couple and the $Mn^{V/IV}$ redox couple occur at potentials of 1.67 and 0.01 V, respectively. These values represent a positive shift of 460 mV for the oxidation process and 370 mV for the reduction process (Table 2). This substantial positive shift for the $Mn^{V/IV}$ redox couple was accompanied by enhanced reactivity as rate measurements of imido group transfer from Mn(Br_8tpfc)(NAr) (**5**) to PEt_3 afforded a second-order rate constant of 3022 ± 61 M^{-1} s^{-1}, over 2 orders of magnitude greater (252×) than that measured for **2** (12.2 ± 0.1 M^{-1} s^{-1}). Despite this significant change in both redox potential and phosphine reactivity, **4** and **5** remained unreactive toward olefins.

The redox potentials for the analogous chromium imido complexes are also given in Table 2 alongside the manganese compounds for comparison. Since the chromium imido complex with chloride substituents on the aryl imido ligand is sufficiently stable, its cyclic voltammogram was measured. While the chloro substituents on the aryl imide have no bearing on the oxidation potential of the corrole ligand (tpfc/tpfc$^{\bullet+}$), they cause a positive shift of 340 mV in the $Mn^{V/IV}$ potential. Hence, the combined effects of brominating the corrole ligand and having chloride substituents on the aryl imide provide a predicted value for the $Mn^{V/IV}$ potential in **5** of 0.35 V. However, this could not be confirmed experimentally due to a lack of stability of **5**.

Synthesis, Characterization, and Reactivity Trends of Chromium(V) Imido Corrole Complexes. Chromium corrole imido complexes were synthesized in a fashion similar to that of the corresponding manganese complexes. Both imido complexes derived from mesityl azide (**6**) and trichlorophenyl azide (**7**) are quite stable in air and can be synthesized using either thermal or photochemical activation of substituted aryl azides. The resulting complexes are easily purified by column chromatography followed by aerobic crystallization from toluene/pentane solvent mixtures. The Cr^{V} oxidation state was confirmed by their room temperature EPR spectra and values of 1.90 μ_B and 1.93 μ_B (1 μ_B = 9.27 × 10^{-24} J T^{-1}) obtained for the paramagnetic susceptibility of **6** and **7**, respectively. These values are slightly greater than the spin-only value for one unpaired electron but in excellent accord with values obtained for chromium(V) nitrido complexes in the literature.[19] Like their manganese counterparts, chromium imido complexes react with triphenylphosphine, resulting in the formation of the phosphine imide adduct, a manifestation of the electrophilic nature of the NR group. For **7** the reaction is complete in 48 h at 85 °C compared with less than 10 min at room temperature for **2**. The additional stability of the imido complexes as an effect of changing the metal from Mn to Cr is best understood in terms of the $Cr^{V/IV}$ and $Mn^{V/IV}$ redox potentials. The $Cr^{V/IV}$ redox couple for **6** is shifted negatively with respect to the $Mn^{V/IV}$ redox couple in the analogous complex **1**. The $Cr^{V/IV}$ potentials in **6** (−0.47 V) and **7** (−0.13 V) are also shifted negatively compared to that of Cr(tpfc)(O) (0.11 V), reflecting the greater π-donating strength of the imido ligand.

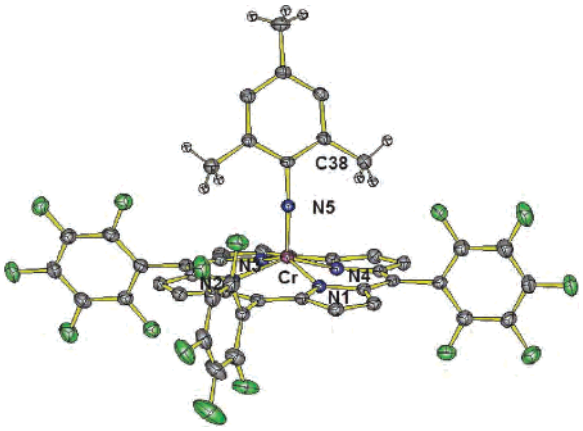

Figure 6. Molecular structure of **6** showing 50% probability ellipsoids and partial atom labeling schemes. Select bond distances and angles are Cr−N1 = 1.955(2) Å, Cr−N2 = 1.941(2) Å, Cr−N3 = 1.943(2) Å, Cr−N4 = 1.932(2) Å, Cr−N5 = 1.635(2) Å, and Cr−N5−C38 = 169.59(18)°.

Differences in the observed reactivities cannot be easily correlated to structural elements of the complexes since the two available structures of **1** and **6** feature similar structural parameters. A discussion of the structure of complex **6** and its comparison to other related structures including that of its manganese analogue complex **1** is undertaken next.

X-ray Molecular Structure of Cr(tpfc)(NMes)·C_7H_8 (6·C_7H_8). The molecular structure of Cr(tpfc)(NMes) (**6**) is shown in Figure 6. The critical distances (Å) and angle (deg) are Cr−N1 = 1.955(2), Cr−N2 = 1.941(2), Cr−N3 = 1.943(2), Cr−N4 = 1.932(2), Cr−N5 = 1.635(2), and Cr−N5−C38 = 169.59(18). The metal−nitrogen pyrrole dis-

(19) (a) Meyer, K.; Bendix, J.; Bill, E.; Weyhermüller, T.; Wieghardt, K. *Inorg. Chem.* **1998**, *37*, 5180. (b) Che, C. M.; Ma, J. X.; Wong, W. T.; Lai, T. F.; Chung, K. P. *Inorg. Chem.* **1988**, *27*, 2547.

Table 3. Comparison of Structural Parameters of **6** to Those of Related Structures

complex	metal displacement from the plane of the macrocycle[a]/Å	M−$N_{pyrrole}$ range/Å	M−L_{axial}[b]/Å	ref
Cr(tpfc)(NMes) (**6**)	0.54	1.932−1.955	1.64	this work
$Cr(tpfc)(py)_2$	0.14	1.926−1.952	2.109, 2.129	11e
Mn(tpfc)(NMes) (**1**)	0.51	1.891−1.947	1.61	8
Cr(tpfc)(O)[c]	0.56	1.936−1.942	1.57	9a
domed	0.57	1.927−1.943	1.57	
twisted				
Cr(tpp)(O)	0.47	2.028−2037	1.572	21

[a] Plane of macrocycle is defined by the four pyrrolic nitrogen atoms. [b] L_{axial} designates the axial ligand. [c] Two conformers exist for this complex in the solid-state structure, one in which all the pyrroles bend downward (*Domed*) and the other in which one of the pyrrole rings bends upward (*Twisted*).

tances are within the range of those of both its isoelectronic counterpart Cr(tpfc)(O)[9a] and the related $Cr^{III}(tpfc)(py_2)$,[11e] while they are slightly longer than those of Mn(tpfc)(NMes).[8] As there is no crystal structure of chromium imido porphyrin,[20] we utilize the structure of a chromium(IV) oxo porphyrin, Cr(tpp)(O), for comparison to **6**.[21] Metal−nitrogen pyrrole distances for Cr(tpp)(O) are longer than those of our corrole complex **6**. This difference between the corrole and the porphyrin complex is almost exclusively due to the different sizes of the ligands. The imido linkage exhibits a short Cr−N distance of 1.635 Å and is almost linear (Cr−N5−C38 = 169.60°), which is consistent with a formal triple bond. The Cr atom is displaced out of the plane as defined by the four pyrrole nitrogen atoms by 0.54 Å. This metal out-of-plane displacement is almost identical to those of the Cr^{V}(tpfc)O conformers (0.56 and 0.57 Å),[9a] slightly greater than that of the Mn(tpfc)(NMes) complex (0.51 Å),[8] and significantly larger than that of the Cr(tpp)O complex (0.47 Å).[21] Shorter metal−nitrogen pyrrole distances and larger metal out-of-plane displacements along with a unique ability to destabilize low-valent metal complexes (through raising the energy of metal d orbitals) are the main factors that have been attributed to the greater stability of corrole complexes over those of porphyrin ligand systems.[9a] The main structural parameters of **6** are compared to those of related structures of porphyrin and corrole macrocycles in Table 3.

Electron Paramagnetic Resonance (EPR) Spectra. The room temperature EPR spectrum of Cr(tpfc)(NAr) (**7**) in toluene (Figure 7) displays a sharp isotropic signal at g_o = 1.987 reflecting the $3d_{xy}^1$ ground-state electronic configuration. It features an intense central resonance of eleven lines attributable to coupling of the unpaired electron to five ^{14}N nuclei, which indicates that all five nitrogen atoms (four pyrrole nitrogens and the axial imido nitrogen) in **7** are magnetically equivalent. This is a recurring phenomenon observed with chromium(V) nitrido complexes and thought to result from Fermi contact or through bond resonances occurring to the same extent.[22] The main signal is flanked

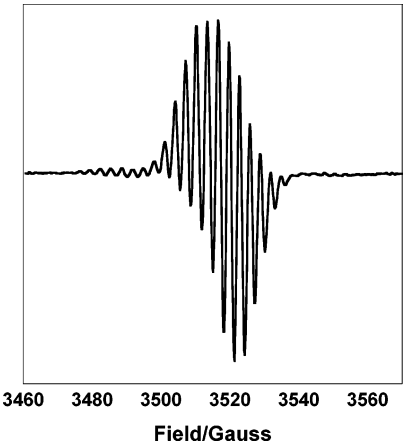

Figure 7. X-band EPR spectrum of Cr(tpfc)(NAr) (**7**) in toluene at 298 K. Experimental conditions: microwave frequency 9.770 GHz, microwave power 2.0 mW, modulation amplitude 1.00 G.

Table 4. EPR Parameters for a Series of Cr(V) Complexes

complex	g_{iso}	A^{53}_{Cr}/mT	A^{14}_{N}/mT
Cr(tpfc)(NAr)[a]	1.987	2.18	0.31
Cr(tpfc)(NMes)[a]	1.985	2.18	0.31
Cr(tpfc)(O)[b]	1.986	1.64	0.30
Cr(tpfc)(N)[c]		2.67	0.27
Cr(salen)(N)[d]	1.978	2.83	0.25
Cr(bpb)(N)[e]	1.982	2.73	0.23
Cr(ttp)(N)[f]	1.985	2.85	0.28
Cr(oep)(N)[f]	1.982	2.83	0.28

[a] This work. [b] Reference 9a. [c] Reference 22. [d] Reference 23. [e] Reference 24. H_2bpb = 1,2-bis((2-pyridylcarboxy)amido)benzene. [f] Reference 25. oep = octaethylporphinate(2−) and ttp = tetratolylporphinate(2−).

on either side by two smaller satellites due to coupling to ^{53}Cr (I = 3/2 and abundance 9.4%). The isotropic hyperfine coupling constants of **6** and **7** were determined to be A^{53}_{Cr} = 2.18 mT and A^{14}_{N} = 0.31 mT.

Table 4 reveals that the EPR parameters determined for **6** and **7** fall within the range of those found for other Cr(V) species based on corrole, porphyrin, and salen ancillary ligands. A comparison of the hyperfine coupling constants for the nitrido, imido, and oxo tpfc complexes is noteworthy: A^{53}_{Cr}/A^{14}_{N} constants (mT) are 2.67/0.27, 2.18/0.31, and 1.64/0.31 for the nitrido, imido, and oxo moieties, respectively. In the case of the oxo complex, these values, a manifestation of the relative spin densities on the metal (low) and ligand (high), have been explained in terms of the strong σ donation from the pyrrole nitrogen atoms to the metal and the subsequent transfer of that electron density to the axial ligand via a π-type donation.[9a] This argument is undoubtedly also applicable to the nitrido, but the strong π-donating ability of this ligand negates the σ-donating effect, resulting in relative spin densities that are much higher on the metal and lower on the ligand than in the oxo and imido counterparts. In our imido complexes, there is interplay of the σ-donating effect of the pyrrolic nitrogens and the π-donating ability of the axial ligand, resulting in spin densities that remain high on the ligand but greater on the metal than in the case of the oxo moiety. The A^{14}_{N} coupling constant, being an effective measure of the σ-donation of the pyrrolic nitrogen atoms to the metal, is greatest for the oxo and imido corrole complexes, leading to short metal−nitrogen pyrrole distances

(20) For chromium(IV) imido porphyrin complexes, see: Moubaraki, B.; Murray, K. S.; Nichols, P. J.; Thomson, S.; West, B. O. *Polyhedron* **1994**, *13*, 485.
(21) Groves, J. T.; Kruper, W. R., Jr.; Haushalter, R. C.; Butler, W. M. *Inorg. Chem.* **1982**, *21*, 1363.
(22) Golubkov, G.; Gross, Z. *Angew. Chem., Int. Ed.* **2003**, *42*, 4507.

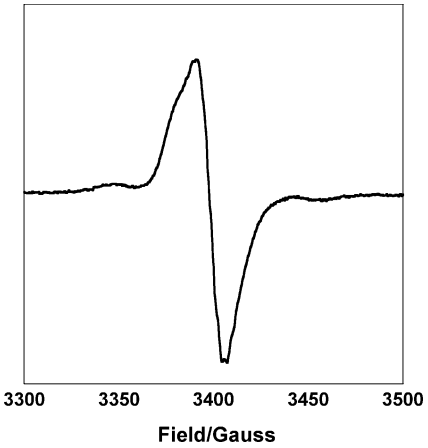

Figure 8. EPR spectrum of Cr(tpfc)(NAr) (**7**) in toluene at 93 K.

and hence complexes that are more stable than those based on salen and porphyrin ancillary ligands.

An anisotropic, in particular, axially symmetric signal was observed for **6** and **7** at 93 K (Figure 8), as has been noted for both chromium(V) nitrido and oxo complexes.[26] It is worth noting that, in going to imido, a weaker π-donating ligand than nitrido, there is a shift to lesser anisotropic behavior in the low-temperature EPR signal.

Conclusions

The first examples of manganese(V) and chromium(V) imido corroles have been prepared and fully characterized. The synthetic methodology relied on the interception by the metalated corrole of aryl nitrene, generated via thermal or photochemical decomposition of the corresponding organic azide. Manganese(V) complexes containing electron-withdrawing substituents on the aryl imide ligand were found to be sufficiently reactive with various organic phosphines, allowing detailed rate measurements. Reduction of manganese(V) to manganese(III) accompanied by nitrene [NR] transfer was sensitive to steric and electronic parameters of the substrate. Modification of the corrole ligand by introducing bromine atoms in the β-pyrrole positions had a pronounced effect on the complex activity as well as caused a significant positive shift of the $Mn^{V/IV}$ electrochemical potential.

An X-ray single-crystal structural analysis of a chromium(V) corrole has been performed. Shorter metal−nitrogen pyrrole distances and larger metal out-of-plane displacements were observed for Cr^{V}(tpfc)(NMes) (**6**) in comparison to a Cr^{IV}=O porphyrin, but within the ranges displayed by other high-valent corrole complexes. The EPR spectra of chromium(V) imido corroles are similar to those of their chromium nitrido analogues and, as expected, are characteristic for a d^1 system with a strong spin localization in the d_{xy} orbital.

Acknowledgment. We thank Dr. Saeed I. Khan for assistance with the crystal structure determination and Dr. Clifton K. F. Shen for assistance with MALDI MS measurements. This work was supported by the NSF.

Supporting Information Available: MALDI-TOF MS for the phosphine imine adducts (tpfc)Mn(NArPPh$_3$), (tpfc)Mn(NArP(4-FC$_6$H$_4$)$_3$), and (tpfc)Mn(NArPCy$_3$) (with instrument parameters) and NMR spectra of complexes **3** and **5** (PDF) and tables of crystal data, structure solution and refinement details, atomic coordinates, bond lengths and angles, and anisotropic thermal parameters for **6** (CIF). This material is available free of charge via the Internet at http://pubs.acs.org.

IC0484506

(23) Azuma, N.; Imori, Y.; Yoshida, H.; Tajima, K.; Li, Y.; Yamauchi, J. *Inorg. Chim. Acta* **1997**, *266*, 29.
(24) Azuma, N.; Ozama, T.; Tsuboyama, S. *J. Chem. Soc., Dalton Trans.* **1994**, 2609.
(25) (a) Buchler, J. W.; Dreher, C.; Lay, K.-L.; Raap, A.; Gersonde, K. *Inorg. Chem.* **1983**, *22*, 879. (b) Groves, J. T.; Takahashi, T.; Butler, W. M. *Inorg. Chem.* **1983**, *22*, 884.
(26) Fujii, H.; Yoshimura, T.; Kamada, H. *Inorg. Chem.* **1997**, *36*, 1122.